

## Investigating the intra-nuclear cascade process using the reaction $^{136}\text{Xe}$ on deuterium at 500 AMeV

J.A. Alcántara-Núñez<sup>1,a</sup>, J. Benlliure<sup>1</sup>, D. Pérez-Loureiro<sup>1</sup>, P. Armbruster<sup>2</sup>, L. Audouin<sup>3</sup>, M. Bernas<sup>3</sup>, A. Boudard<sup>4</sup>, E. Casarejos<sup>1</sup>, T. Enqvist<sup>2</sup>, B. Fernández-Domínguez<sup>4</sup>, M. Fernández Ordóñez<sup>1</sup>, A. Heinz<sup>2,5</sup>, V. Henzl<sup>2</sup>, D. Henzlova<sup>2</sup>, A. Kelić<sup>2</sup>, A. Lafriashk<sup>3</sup>, S. Leray<sup>3</sup>, P. Napolitani<sup>2,3</sup>, J. Pereira<sup>1</sup>, R. Pleskač<sup>2</sup>, F. Rejmund<sup>3,6</sup>, M.V. Ricciardi<sup>2</sup>, C. Stéphan<sup>3</sup>, K.-H. Schmidt<sup>2</sup>, C. Schmitt<sup>2</sup>, L. Tassan-Got<sup>3</sup>, C. Villagrasa<sup>4</sup>, C. Volant<sup>4</sup>, and O. Yordanov<sup>2</sup>

<sup>1</sup> Universidade de Santiago de Compostela, Santiago de Compostela, Spain

<sup>2</sup> Gesellschaft für Schwerionenforschung, 64291 Darmstadt, Germany

<sup>3</sup> IPN Orsay, Université Paris-Sud 11, CNRS/IN2P3, 91406 Orsay Cedex, France

<sup>4</sup> DAPNIA/SPhN, DSM-CEA, 91191 Gif-sur-Yvette Cedex, France

<sup>5</sup> A.W. Wright Nuclear Structure Laboratory, Yale University, New Haven, Connecticut 06511, USA

<sup>6</sup> GANIL, CEA/DSM-CNRS/IN2P3, BP. 55027, 14076 Caen Cedex 5, France

**Abstract.** More than 600 residual nuclei, formed in the spallation of  $^{136}\text{Xe}$  projectiles impinging on deuterium at 500 AMeV of incident energy, have been unambiguously identified and their production cross sections have been determined with high accuracy. By comparing these data to others previously measured for the reactions  $^{136}\text{Xe} + p$  at 1 AGeV and  $^{136}\text{Xe} + p$  at 500 AMeV we investigated the role that neutrons play in peripheral collisions and to understand the energy dissipation in frontal collisions in spallation reactions.

### 1 Introduction

In the last decade, great efforts have been made in order to understand the spallation process. This interest is not only important for their implications in understanding the dynamics of nuclear matter, also for their applications as a neutron source for solid-state physics or material-science investigations [1], radioactive ion beam source [2], also as a form of energy production and nuclear-waste transmutation in accelerator-driven systems [3]. The accurate measurement of isotopic production cross sections of residual nuclei produced in spallation reactions is a fundamental tool used for investigating the energy dissipation mechanism and the dynamics of hot nuclei [4].

Many reactions, using different projectiles ( $^{238}\text{U}$ ,  $^{136}\text{Xe}$ , ...) and targets ( $p$ ,  $d$ , ...) at different incident energies have been investigated in order to better understand the spallation process. In this work, the isotopic production of the residual nuclei issued in collisions of  $^{136}\text{Xe}$  projectiles at 500 AMeV on a deuterium target has been measured. The comparison of these results to previously measured reactions as  $^{136}\text{Xe} + p$  at 1 AGeV [5], and  $^{136}\text{Xe} + p$  at 500 AMeV [6], allow us to investigate and better understand the role that neutrons play in spallation reactions as well as the energy dissipation mechanism.

---

<sup>a</sup> e-mail: [juan.alcantara@usc.es](mailto:juan.alcantara@usc.es)

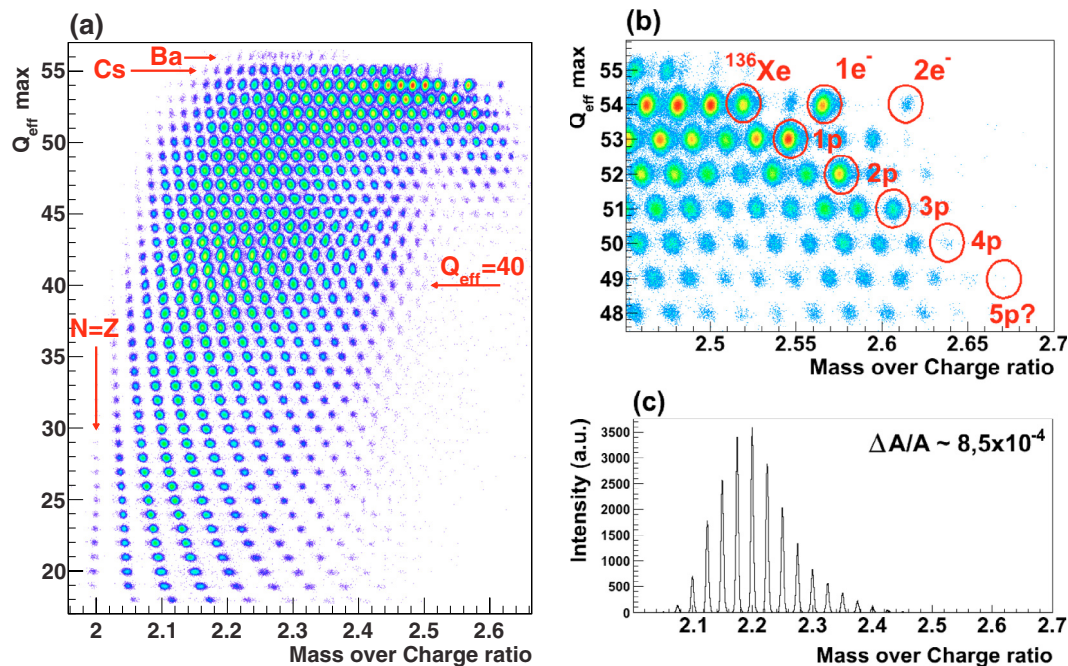


**Fig. 1.** (Color online) (a) Two-dimensional scatter plot of the energy loss of the nuclei transmitted through the FRS vs their  $A/q$  value obtained from the magnetic rigidity and time-of-flight measurements. The production of cesium and barium isotopes are indicated. (b) The primary beam, fully stripped and carrying one electron  $1e^-$ , as well as the proton-loss channel ( $1p$ ,  $2p$ , ...) are indicated. (c) Mass resolution from the nucleus in the matrix identification ( $Q_{eff}^{max} = 40$ ).

## 2 Experiment

The experiment was performed at the GSI facilities, where the SIS18 synchrotron was used to accelerate the  $^{136}\text{Xe}$  beam to 500 AMeV. The average intensity of the beam pulse was  $10^9$  ions/spill, with a duration of 6 s and total cycle time of 10 s. A secondary-electron monitor [7] registered continuously the beam intensity for normalization purposes. The beam impinged onto a liquid deuterium target located at the entrance of the Fragment Separator (FRS) [8]. The liquefied deuterium, with a thickness of  $200 \text{ mg/cm}^2$ , was encapsulated in a Ti container and surrounded by Mylar-Al for thermal isolation. Due to the inverse kinematics, the projectile residues produced in the reaction were emitted in the forward direction and could be analyzed in-flight with the magnetic spectrometer. The resolving power of this device is  $\Delta B\rho/B\rho \sim 1500$  with an angular acceptance of 15 mrad around the beam axis and a momentum acceptance of  $\pm 1.5\%$  [9].

In order to identify all the transmitted nuclei, their horizontal positions at the intermediate and final image planes, their velocity, and their energy loss in a gas volume were measured with different detectors. The measurement of the positions of the fragments at the intermediate and final focal planes with two plastic scintillators [10] defines the magnetic rigidity  $B\rho$ . These detectors also provided the time of flight of the transmitted nuclei between these two image planes. The atomic number of each residual nucleus was determined from its energy loss in two multisampling ionization chambers (MUSICS) [11] placed at the end of the FRS.

In order to measure all the residual nuclei produced in this reaction, and due to the limited acceptance of the FRS, 29 different magnetic tunings of the spectrometer were required. Figure 1a combines these settings in a single identification matrix showing more than 600 different residual nuclei identified in this reaction, and it also shows the production of barium and cesium isotopes. All these nuclei are produced in charge-exchange reactions [12]. In Fig. 1b we can easily identify and separate the first four proton-removal channels ( $1p$ ,  $2p$ , ...) from  $^{136}\text{Xe}$  ( $^{135}\text{I}$ ,  $^{134}\text{Te}$ , ...). The excellent mass resolution obtained in this experiment is illustrated in Fig. 1c.

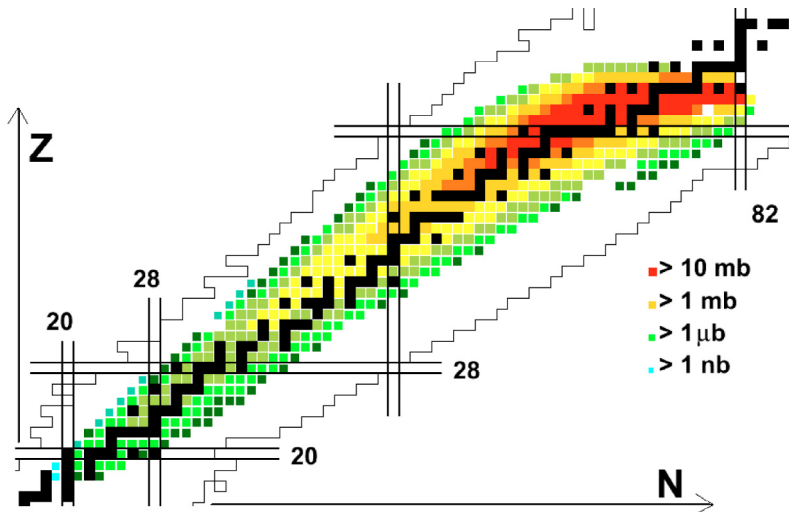


**Fig. 2.** (Color online) Residual nuclei produced in the reaction  $^{136}\text{Xe} + \text{deuterium}$  at 500 MeV per nucleon on top of a chart of nuclide. The color scale represents the production cross section, the black square corresponds to stable isotopes, and the lines indicate the limit of the known nuclides.

### 3 Results

The final production cross sections of the different projectile residues were obtained from the production yields normalized to the number of incident projectiles and the number of the atoms per surface unit of the target. Due to the limited longitudinal momentum acceptance of the FRS, most of the residues were measured in different magnetic settings. By overlapping consecutive settings, the entire momentum distributions of all residues were reconstructed.

The measured yields ( $y_m$ ) evaluated from the complete momentum distributions, were corrected for different effects inherent to the experimental method and data analysis according to Eq. 1. In this equation,  $f_{trans}$ ,  $f_{dead}$ ,  $f_{ch.st}$ ,  $f_{mult}$  and  $f_{sec}$  are the correction factors to take into account due to the transmission through the FRS, the dead time of the data acquisition, the ionic charge state, the multiple reactions within the target and the secondary reactions in all layers of matter along the FRS, respectively. Moreover, in the case of a liquid target, the production is affected by the titanium window of the vessel that contains the target and the Mylar-Al used as thermal insulator ( $y_{dummy}$ ). In order to subtract this contributions, different measurements with the empty container have been made.

$$y_{real} = (y_m - y_{dummy}) \cdot f_{trans} \cdot f_{dead} \cdot f_{ch.st} \cdot f_{mult} \cdot f_{sec} \quad (1)$$

Figure 2 shows the summary of the isotopic cross-section of all the fragments produced in the reaction. More than 600 nuclei were unambiguously identified. The production cross sections of the residues are shown by the color scale. A detailed description of the experimental technique and data analysis procedure can be found in references [13–15].

### 4 Analysis and discussion

In order to describe the interactions of deuterons and protons with  $^{136}\text{Xe}$  at relativistic energy two intra-nuclear cascade codes (INCL4 [16] and ISABEL [17]) have been used. Both codes have been coupled to a de-excitation code (ABLA [18], statistical evaporation and fission model based in the Weisskopf-Ewing formalism). In the intra-nuclear cascade codes, the nuclear reactions are treated as a series of individual nucleon-nucleon interactions assuming quantum considerations as the Pauli blocking. The difference between the two INC codes lies in how the nuclear medium is treated. INCL4 is called the Cugnon-like code where the nucleons are treated individually, and ISABEL is called the Bertini-like code where the nuclear density is considered continuous.

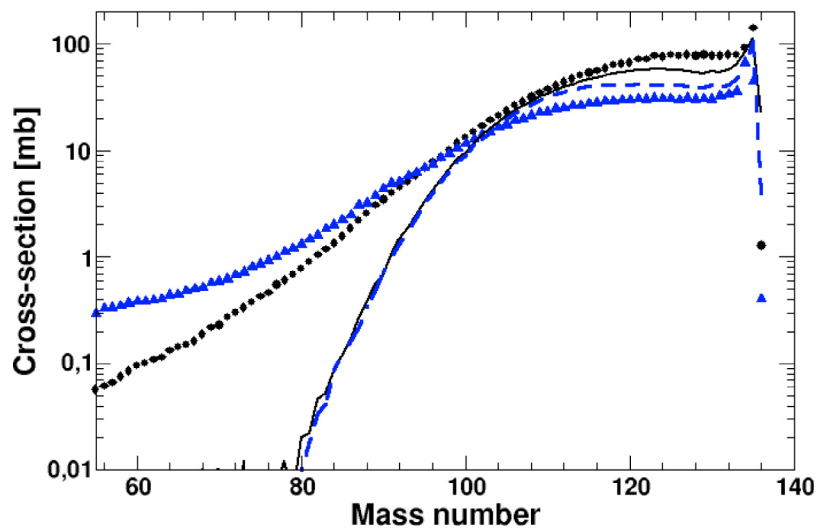


**Fig. 3.** (Color online) Measured isobaric distribution of the residues produced in the reactions  $^{136}\text{Xe}$  (1 AGeV) +  $p$  (triangle),  $^{136}\text{Xe}$  (500 AMeV) +  $d$  (circle) and the isobaric distribution for the same reactions, obtained with the INCL4 intra nuclear cascade code coupled to the ABLA evaporation code. The black line and the blue dashed line are the results obtained with INCL4+ABLA code, for the reaction  $^{136}\text{Xe}$  (1 AGeV) +  $p$ , and  $^{136}\text{Xe}$  (500 AMeV) +  $d$ , respectively.

The large amount of measured data allows the reconstruction of the isobaric distribution of the production cross section. In Fig. 3 we compare the isobaric distributions of residues produced in the reactions  $^{136}\text{Xe}$  (1 AGeV) +  $p$  [5],  $^{136}\text{Xe}$  (500 AMeV) +  $d$  to the prediction obtained with the INCL4 + ABLA code. This comparison could be used to investigate the energy deposition and the nature of in-medium nucleon-nucleon collisions in spallation reactions.

The isobaric distributions of the residual nuclides produced in these two reactions, present a very different pattern: For peripheral collisions (small mass losses), the production cross sections of residual nuclei produced in reactions induced by protons at 1 GeV are smaller than reactions induced by deuterons at 500 MeV. For residual nuclei having similar masses than the projectile (peripheral collisions), we expect that only one of the two nucleons of deuterium hits the  $^{136}\text{Xe}$  nucleus. Since the energy deposition induced by 500 MeV nucleons will be smaller than the energy deposition induced by 1 GeV protons, the cross section of residual nuclei produced in short evaporation chains (small mass losses) will be higher. Theoretical calculations confirm this interpretation.

On the other hand, the same energy deposition is expected for the two systems in frontal collisions. One nucleon at 1 GeV is expected to be equivalent to 2 nucleons at 500 MeV, as shown from theoretical calculations (see the lines in Fig. 3). Surprisingly we observe that collisions induced by 1 GeV proton seems to induce larger energy deposition than collisions produced by 500 MeV deuterons.

For large mass losses, theoretical calculation underestimates the measured cross sections. This behavior could be explained because the production of intermediate mass fragments is not implemented in the version of the ABLA code used in this work. The full understanding of the isobaric distributions for the lighter residues will require advanced model calculations including the emission of intermediate mass fragments as in the new version of ABLA code (ABLA07 [19]).

The analysis of the shape of the isotopic distribution, for the systems mentioned before, shows the influence of the different reaction channels involved in the production of the final nuclei (Fig. 4). In general, the shape of the isotopic distributions for the three reactions we compare are similar. However, the cross sections obtained at 1 AGeV are smaller than the values obtained at 500 AMeV, as already observed in the isobaric distributions.

In the charge exchange channel ( $^{136}\text{Cs}$ ), the production cross section induced by protons at 500 MeV is the same order of magnitude as the production induced by deuterons at the same energy. This result shows a good agreement from a qualitative point of view, to the calculations using INCL4 + ABLA,

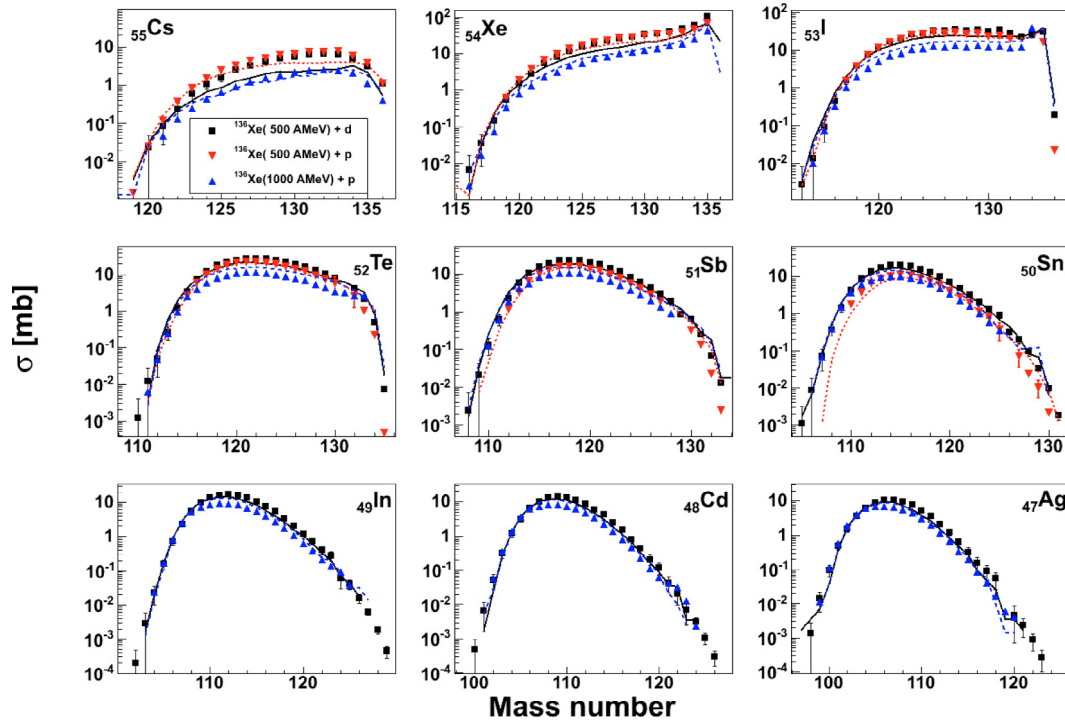


**Fig. 4.** (Color online) The isotopic cross-section of residual nuclei  $_{47}\text{Ag}$  to  $_{56}\text{Cs}$  produced in the reactions  $^{136}\text{Xe}$  (1 AGeV) +  $p$  (blue up-triangle),  $^{136}\text{Xe}$  (500 AMeV) +  $p$  (red down-triangle),  $^{136}\text{Xe}$  (500 AMeV) +  $d$  (black square) compared to the theoretical calculations performed with INCL4 coupled to ABLA evaporation code. The blue dashed, red dot and black solid lines are the results obtained with INCL4 + ABLA code for the reactions  $^{136}\text{Xe}$  (1A GeV) +  $p$ ,  $^{136}\text{Xe}$  (500 AMeV) +  $p$ ,  $^{136}\text{Xe}$  (500 AMeV) +  $d$ , respectively.

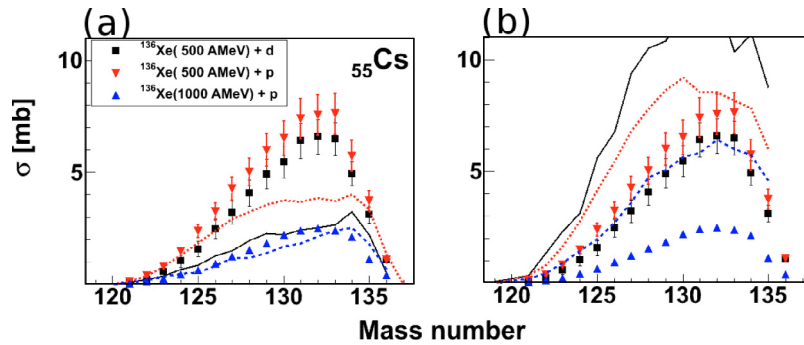


**Fig. 5.** (Color online) Comparison of the isotopic cross-section of charge exchange channel ( $^{136}\text{Cs}$ ) produced in the reactions  $^{136}\text{Xe}$  (1A GeV) +  $p$  (blue up-triangle),  $^{136}\text{Xe}$  (500 AMeV) +  $p$  (red down-triangle),  $^{136}\text{Xe}$  (500 AMeV) +  $d$  (black square) to, (a) INCL4 coupled to ABLA evaporation code, (b) ISABEL coupled to ABLA evaporation code.

but the values are underestimated. On the other hand, the calculations using ISABEL + ABLA show discrepancies. The theoretical values for the three system are overestimate. Looking more carefully at the charge-exchange channel, is possible to observe a small difference in the isotopic distribution. The production cross sections present lower values with the deuterium than with the proton target (see Fig. 5). This difference is due to the fact the neutron inside the deuterium do not contribute with elastic charge-exchange processes to the production of Cs isotopes.

## 5 Summary

The accurate measurement of isotopic production cross sections of the residues provides relevant information on the spallation reactions. In particular, in this work, more than six hundred nuclei produced in reactions induced by  $^{136}\text{Xe}$  projectiles at 500 AMeV on a deuterium target has been identified. Comparisons with results from other reactions previously measured, have been used to investigate the energy deposition and the nature of in-medium nucleon-nucleon collisions in spallation reactions. From the analysis of the isobaric distributions, for peripheral collisions, INCL4 + ABLA code shows a good agreement, from a qualitative point of view, to the experimental results. For frontal collisions, the results show the opposite to the expected values and to intra-nuclear cascade simulation codes; two nucleons at 500 AMeV deposit less energy in the target nucleus than a single proton at 1000 AMeV. The comparison of the isotopic distributions of residual nuclei close to the projectile shows a larger production for reactions induced by  $^{136}\text{Xe}$  projectiles on protons at 500 AMeV than on deuterium at the same energy. This observation is explained by the fact that the neutron inside the deuterium does not contribute to any elastic charge-exchange process. Other analyses are necessary to understand the role that the neutron plays in the reaction with a deuterium target.

## References

1. *Review of the Spallation Neutron Source (SNS)*, DOE/ER-0705 (1997).
2. *Proceeding of the Sixth International Conference on Radioactive Nuclea Beam* (Argonne, USA 2003), Nucl. Phys. **A748**, (2005).
3. T. Takisuka, *Proceeding of the International Conference on Accelerator-Driven Transmutation Tecnologies and Aplications* (AIP conference proceedings, Las Vegas 1994).
4. J. Benlliure, *The Euroschool lecture on Physics With Exotic Beams, Vol. II* (Springer-Verlag, Berlin Heidelberg 2006) 191–234.
5. P. Napolitani, et al., Phys. Rev. **C76**, (2007) 064609.
6. C. Paradela, et al., in *Proceeding of the International Conference on Nuclear Data for Science and Technology* (2007).
7. A.R Junghans, et al., Nucl. Instrum. Methods **A370**, (1996) 312.
8. H. Geissel, et al., Nucl. Instrum. Methods **B70**, (1992) 286.
9. J. Benlliure, et al., Nucl. Instrum. Methods **A478**, (2002) 493.
10. B. Voss, et al., Nucl. Instrum. Methods **A364**, (1995) 150.
11. M. Pfützner, et al., Nucl. Instrum. Methods **B86**, (1994) 213.
12. A. Kelic, et al., Phys. Rev. **C70**, (2004) 064608.
13. E. Casarejos, et al., Phys. Rev. **C77**, (2004) 044612.
14. J. Benlliure, et al., Nucl. Phys. **A660**, (1999) 87.
15. J. Benlliure, et al., Phys. Rev. **C78**, (2008) 054605.
16. A. Boudard, et al., Phys. Rev. **C66**, (2002) 044615.
17. Y. Yariv and Z. Freankel, Phys. Rev. **C20**, (1979) 2227.
18. J.-J. Gaimard, et al., Nucl. Phys. **A531**, (1991) 187.
19. M. Valentina Ricciardi, in *Proceeding of the International Conference on Nuclear Data for Science and Technology* (2007).